

Harvesting correlations from vacuum quantum fields in the presence of a reflecting boundary

Zhihong Liu¹, Jialin Zhang^{1,2} *and Hongwei Yu^{1,2} †

¹ *Department of Physics and Synergetic Innovation Center for Quantum Effects and Applications, Hunan Normal University, 36 Lushan Rd., Changsha, Hunan 410081, China*

² *Institute of Interdisciplinary Studies, Hunan Normal University, 36 Lushan Rd., Changsha, Hunan 410081, China*

(Dated: October 12, 2023)

Abstract

We explore correlations harvesting by two static detectors locally interacting with vacuum massless scalar fields in the presence of an infinite perfectly reflecting boundary. We study the phenomena of mutual information harvesting and entanglement harvesting for two detector-boundary alignments, i.e., parallel-to-boundary and vertical-to-boundary alignments. Our results show that the presence of the boundary generally inhibits mutual information harvesting relative to that in flat spacetime without any boundaries. In contrast, the boundary may play a doubled-edged role in entanglement harvesting, i.e., inhibiting entanglement harvesting in the near zone of the boundary while assisting it in the far zone of the boundary. Moreover, there exists an optimal detector energy gap difference between two nonidentical detectors that makes such detectors advantageous in correlations harvesting as long as the interdetector separation is large enough. The value of the optimal detector energy gap difference depends on both the interdetector separation and the detector-to-boundary distance. A comparison of the correlations harvesting in two different alignments shows that although correlations harvesting share qualitatively the same properties, they also display quantitative differences in that the detectors in vertical-to-boundary alignment always harvest comparatively more mutual information than the parallel-to-boundary ones, while they harvest comparatively more entanglement only near the boundary.

* Corresponding author at jialinzhang@hunnu.edu.cn

† Corresponding author at hwyu@hunnu.edu.cn

I. INTRODUCTION

It has been recognized for a long time that the vacuum state of free quantum fields possesses nonlocal properties and contains correlations between timelike and spacelike separated regions [1–4]. Such correlations, which may be either quantum entanglement, quantum mutual information or quantum discord [5], can be extracted by a pair of initially uncorrelated Unruh-DeWitt (UDW) particle detectors interacting with the vacuum quantum fields. This phenomenon has been known as correlation harvesting, and such harvesting process is referred to as the correlation harvesting protocol [3].

The correlation harvesting in terms of quantum entanglement has been extensively studied in different circumstances in recent years and has been demonstrated to be sensitive to the properties of spacetime including dimensionality [3], topology [6], curvature [4, 7–14] and the presence of boundaries [15–17], the intrinsic motion and energy gap of detectors [16, 18–23], and superpositions of temporal order for detectors [24].

Recently, the study of entanglement harvesting has been extended to nonidentical detectors with different energy gaps in flat spacetime [25], in contrast to previous studies where detectors are usually assumed to be identical. It was argued that the presence of energy gap difference generally enlarges the rangefinding of entanglement harvesting (the harvesting-achievable range for the interdetector separation), and two nonidentical detectors can harvest more entanglement than the identical ones if the interdetector separation is not too small with respect to the interaction duration time. However, the validity of such results in other circumstances such as in curved spacetime or in the presence of boundaries merits further exploration. In fact, it has been recognized that the presence of reflecting boundaries in flat spacetime modifies the fluctuations of quantum fields, resulting in some intriguing quantum effects, such as the Casimir effect [26], the light-cone fluctuations [27], the geometric phase [28] and the modification for the radiative properties of accelerated atoms [29–31]. Since the dynamic evolution in time of the detectors system is strongly dependent on the fluctuations of quantum fields, modifications of the fields fluctuations caused by the presence of a boundary have been shown to play a significant role in controlling the entanglement creation in the detectors system [32–34]. And the phenomena of entanglement harvesting by two UDW detectors locally interacting with the fluctuating quantum fields have also been examined in the presence of a reflecting boundary but in a simple scenario:

two identical detectors with not too large energy gap in parallel-to-boundary alignment [16]. It was found, through the numerical evaluation, that the reflecting boundary plays a double-edged role in entanglement harvesting, i.e., degrading the harvested entanglement amount in general while enlarging the entanglement harvesting-achievable interdetector separation range. However, what happens to the entanglement harvesting phenomenon in the presence of a boundary when detectors are nonidentical remains to be investigated.

On the other hand, the correlation harvesting in terms of mutual information, a useful measure on information which quantifies the total amount of classical and quantum correlations including entanglement, has also been recently studied. It has been found that the mutual information harvesting also depends upon the intrinsic properties of spacetime, the detectors' energy gap and noninertial motion [3, 5, 35, 36]. Remarkably, unlike the entanglement harvesting that has a finite harvesting-achievable separation range and cannot occur near a black hole, mutual information harvesting can occur everywhere with an arbitrarily large interdetector separation [3] and even does not vanish near the event horizon of a black hole at an extremely high local Hawking temperature [36]. However, in comparison to the entanglement harvesting which is relatively well understood, much remains to be done on understanding the phenomenon of mutual information harvesting, for an example, the mutual information harvesting by two identical/nonidentical detectors near a boundary.

In this paper, we will perform a general study of the correlation harvesting phenomenon for two detectors placed near a reflecting boundary, focusing upon entanglement harvesting and mutual information harvesting phenomenon by nonidentical detectors. Our particular interest lies in the influence of energy gaps on mutual information harvesting and the role played by a perfectly reflecting plane boundary, including correlation harvesting by non-identical detectors with different energy gaps in the scenarios of parallel-to-boundary and vertical-to-boundary alignments.

The paper is organized as follows. We begin in section II by briefly reviewing the UDW detector model, the correlation harvesting protocol, and introduce the conventional measures for entanglement and mutual information. In section III, we respectively explore the phenomena of entanglement harvesting and mutual information harvesting for two static detectors aligned parallel to the boundary, where the influence of the boundary and detectors' energy gaps on correlation harvesting will be studied in detail, and make a qualitative comparison between the phenomena of mutual information harvesting and entanglement

harvesting. In section IV, the correlation harvesting phenomenon for detectors aligned vertically to the boundary will be studied, and some comparisons of the results between the parallel-to-boundary and the vertical-to-boundary alignments are made. Finally, we end with conclusions in section V. Throughout the paper, the natural units $\hbar = c = k_B = 1$ are adopted for convenience.

II. THE BASIC FORMALISM

We consider two detectors A and B locally interacting with a massless quantum scalar field $\phi[x_D(\tau)]$ ($D \in \{A, B\}$) along their worldlines. The spacetime trajectory of the detector, $x_D(\tau)$, is parametrized by its proper time τ . The detector-field coupling is given by the following interaction Hamiltonian

$$H_D(\tau) = \lambda \chi(\tau) [e^{i\Omega_D \tau} \sigma^+ + e^{-i\Omega_D \tau} \sigma^-] \phi[x_D(\tau)], \quad D \in \{A, B\}, \quad (1)$$

where λ is the coupling strength, and $\chi(\tau) = \exp[-\tau^2/(2\sigma^2)]$ is the Gaussian switching function with parameter σ controlling the duration time of the interaction. In principle, all relevant physical quantities can be rescaled with the duration time parameter σ to be unitless. Here, we use the standard UDW detector model to describe a two-level system with an energy gap Ω_D between its ground state $|0\rangle_D$ and excited state $|1\rangle_D$. The operators $\sigma^+ = |1\rangle_D \langle 0|_D$ and $\sigma^- = |0\rangle_D \langle 1|_D$ are just the SU(2) ladder operators.

Suppose the two detectors are prepared in their ground state and the field is in the Minkowski vacuum state $|0\rangle_M$, then the initial state of the two detectors and field system is given by $|\Psi\rangle_i = |0\rangle_A |0\rangle_B |0\rangle_M$. The time-evolution of the quantum system can be obtained by using the Hamiltonian (1),

$$|\Psi\rangle_f := \mathcal{T} \exp \left[-i \int dt \left(\frac{d\tau_A}{dt} H_A(\tau_A) + \frac{d\tau_B}{dt} H_B(\tau_B) \right) \right] |\Psi\rangle_i, \quad (2)$$

where \mathcal{T} is the time ordering operator and t is the coordinate time with respect to which the vacuum state of the field is defined. By tracing out the field degrees of freedom in Eq. (2), the density matrix for the final state of the two detectors turns, to leading order in the interaction strength and in the basis $\{|0\rangle_A |0\rangle_B, |0\rangle_A |1\rangle_B, |1\rangle_A |0\rangle_B, |1\rangle_A |1\rangle_B\}$, out to

be [3, 12]

$$\begin{aligned} \rho_{AB} &:= \text{tr}_\phi (U |\Psi_f\rangle \langle \Psi_f| U^\dagger) \\ &= \begin{pmatrix} 1 - P_A - P_B & 0 & 0 & X \\ 0 & P_B & C & 0 \\ 0 & C^* & P_A & 0 \\ X^* & 0 & 0 & 0 \end{pmatrix} + \mathcal{O}(\lambda^4), \end{aligned} \quad (3)$$

where the detector transition probability reads

$$P_D := \lambda^2 \iint d\tau d\tau' \chi(\tau) \chi(\tau') e^{-i\Omega_D(\tau-\tau')} W(x_D(t), x_D(t')) \quad D \in \{A, B\}, \quad (4)$$

and the quantities C and X which characterize correlations of the two detectors, are given by

$$C := \lambda^2 \iint d\tau d\tau' \chi(\tau) \chi(\tau') e^{-i(\Omega_A \tau - \Omega_B \tau')} W(x_A(t), x_B(t')), \quad (5)$$

$$\begin{aligned} X &:= -\lambda^2 \iint d\tau d\tau' \chi(\tau) \chi(\tau') e^{-i(\Omega_A \tau + \Omega_B \tau')} \left[\theta(t' - t) W(x_A(t), x_B(t')) \right. \\ &\quad \left. + \theta(t - t') W(x_B(t'), x_A(t)) \right]. \end{aligned} \quad (6)$$

Here $W(x, x') := \langle 0|_M \phi(x) \phi(x') |0\rangle_M$ is the Wightman function of the quantum field in the Minkowski vacuum state, and $\theta(t)$ is the Heaviside theta function. In particular, if detectors are at rest, one has $t = \tau$, i.e., the coordinate time of the detector is equal to its proper time. The amount of quantum entanglement can be measured by concurrence [37], which, with the density matrix (3), is given by [6, 11, 12]

$$\mathcal{C}(\rho_{AB}) = 2 \max \left[0, |X| - \sqrt{P_A P_B} \right] + \mathcal{O}(\lambda^4). \quad (7)$$

Obviously, the concurrence is a competition between the correlation term X and geometric mean of the detectors' transition probabilities P_A and P_B . The total amount of correlations is characterized by mutual information, which is defined as [38]

$$\mathcal{I}(\rho_{AB}) = S(\rho_A) + S(\rho_B) - S(\rho_{AB}), \quad (8)$$

where $\rho_A = \text{tr}_B(\rho_{AB})$ and $\rho_B = \text{tr}_A(\rho_{AB})$ denote the partial traces of detectors' state ρ_{AB} , and $S(\rho) = -\text{tr}(\rho \ln \rho)$ is the von Neumann entropy. With the above definition (8), the mutual information for the final detector state (3) takes the following form [3]

$$\mathcal{I}(\rho_{AB}) = \mathcal{L}_+ \ln(\mathcal{L}_+) + \mathcal{L}_- \ln(\mathcal{L}_-) - P_A \ln(P_A) - P_B \ln(P_B) + \mathcal{O}(\lambda^4) \quad (9)$$

with

$$\mathcal{L}_\pm = \frac{1}{2} \left(P_A + P_B \pm \sqrt{(P_A - P_B)^2 + 4|C|^2} \right). \quad (10)$$

In contrast to the concurrence (7), the mutual information is determined by transition probabilities P_A , P_B and the correlation term C rather than the correlation term X . It can be verified that mutual information is an increasing function of parameter $|C|$, and monotonically decreases as the transition probabilities increase. According to Eq. (9), we can further obtain $\mathcal{I}(\rho_{AB}) = 0$ if $C = 0$. Especially, when a transition probability is zero, the mutual information must vanish from the positivity condition of the density matrix, (i.e., $P_A P_B \geq |C|^2$).

In what follows, we will explore, with the harvesting protocol, the correlations harvested by two static detectors near a perfectly reflecting boundary, figuring out the role played by the presence of the boundary in both entanglement harvesting and mutual information harvesting. It is supposed that a perfectly reflecting plane boundary is located at $z = 0$, and two nonidentical UDW detectors with different energy gaps are aligned in two different ways: parallel-to-boundary and vertical-to-boundary.

III. CORRELATION HARVESTING FOR THE DETECTORS ALIGNED PARALLEL TO THE BOUNDARY

In section, we consider that two static detectors separated by a distance L are aligned parallel to the boundary with a distance Δz from the boundary (see Fig. (1)). The spacetime trajectories of the detectors can then be written as

$$x_A := \{t_A, x = 0, y = 0, z = \Delta z\}, \quad x_B := \{t_B, x = L, y = 0, z = \Delta z\}. \quad (11)$$

Let us now calculate the transition probabilities P_D given by Eq. (4) and the correlation terms C and X respectively given by Eq. (5) and Eq. (6). To do this, we need the Wightman function for vacuum massless scalar fields, which is, according to the method of images, given by [39]

$$W(x_D, x'_D) = -\frac{1}{4\pi^2} \left[\frac{1}{(t - t' - i\epsilon)^2 - (x - x')^2 - (y - y')^2 - (z - z')^2} \right. \\ \left. - \frac{1}{(t - t' - i\epsilon)^2 - (x - x')^2 - (y - y')^2 - (z + z')^2} \right]. \quad (12)$$

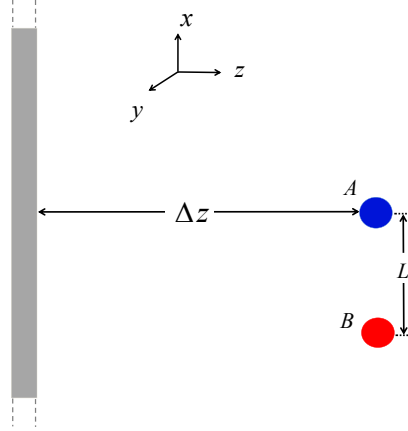


FIG. 1: Two static detectors separated from each other by a distance L are aligned parallel to the boundary at a distance Δz away from the boundary.

Substituting trajectory (11) and Eq. (12) into Eq. (4), one may straightforwardly obtain the transition probabilities [16]

$$P_D = \frac{\lambda^2}{4\pi} \left[e^{-\Omega_D^2 \sigma^2} - \sqrt{\pi} \Omega_D \sigma \text{Erfc}(\Omega_D \sigma) \right] - \frac{\lambda^2 \sigma e^{-\Delta z^2/\sigma^2}}{8\sqrt{\pi} \Delta z} \times \left\{ \text{Im} \left[e^{2i\Omega_D \Delta z} \text{Erf} \left(i \frac{\Delta z}{\sigma} + \Omega_D \sigma \right) \right] - \sin(2\Omega_D \Delta z) \right\}, \quad D \in \{A, B\}, \quad (13)$$

where $\text{Erf}(x)$ is the error function and $\text{Erfc}(x) := 1 - \text{Erf}(x)$. Similarly, the correlation terms C and X in this case can also be worked out

$$C = \frac{\lambda^2}{4\sqrt{\pi}} e^{-\frac{\Delta\Omega^2 \sigma^2}{4}} \left[f(L) - f(\sqrt{L^2 + 4\Delta z^2}) \right], \quad (14)$$

$$X = -\frac{\lambda^2}{4\sqrt{\pi}} e^{-\frac{(2\Omega_A + \Delta\Omega)^2 \sigma^2}{4}} \left[g(L) - g(\sqrt{L^2 + 4\Delta z^2}) \right], \quad (15)$$

where the auxiliary functions, f and g , are defined by

$$f(L) := \frac{\sigma e^{-L^2/(4\sigma^2)}}{L} \left\{ \text{Im} \left[e^{i(2\Omega_A + \Delta\Omega)L/2} \text{Erf} \left(\frac{iL + 2\Omega_A \sigma^2 + \Delta\Omega \sigma^2}{2\sigma} \right) \right] - \sin \left[\frac{(2\Omega_A + \Delta\Omega)L}{2} \right] \right\}, \quad (16)$$

and

$$g(L) := \frac{\sigma e^{-L^2/(4\sigma^2)}}{L} \left\{ \text{Im} \left[e^{i\Delta\Omega L/2} \text{Erf} \left(\frac{iL + \Delta\Omega \sigma^2}{2\sigma} \right) \right] + i \cos \left(\frac{\Delta\Omega L}{2} \right) \right\}. \quad (17)$$

Without loss of generality, we here assume the energy gap of the detector B is not less than that of detector A , i.e., $\Delta\Omega := \Omega_B - \Omega_A \geq 0$ throughout the paper. From Eq. (14) and

Eq. (15), it is easy to find that as long as the energy gap difference is large with respect to duration time parameter ($\Delta\Omega \gg 1/\sigma$), both the correlation terms C and X become vanishingly small, and so mutual information and entanglement can hardly be harvested.

A. Entanglement harvesting

In general, it is very difficult to capture the characteristics of the correlation harvesting phenomena with the very complicated analytical results above. So, the numerical evaluations are usually called for investigating the influence of the boundary and the energy gaps on correlation harvesting. However, in some special cases, one can still perform analytical approximations to the afore-results. For two identical detectors, i.e., $\Omega_A = \Omega_B = \Omega$, the approximate results for harvested entanglement can be derived in two cases: small energy gap ($\Omega\sigma \ll 1$) and large energy gap ($\Omega\sigma \gg 1$).

1. Small energy gap

When the detectors system is very close the boundary (i.e., $\Delta z/\sigma \ll 1$), the transition probabilities can be approximated as

$$P_A = P_B \approx \frac{\lambda^2 \Delta z^2}{2\pi\sigma^2} \left(\frac{1}{3} - \frac{\sqrt{\pi}\Omega\sigma}{2} \right), \quad (18)$$

and the correlation term $|X|$ as

$$|X| \approx \begin{cases} \frac{\lambda^2 \Delta z^2 \sigma}{2L^3 \sqrt{\pi}} (1 - \Omega^2 \sigma^2), & \frac{L}{\sigma} \ll 1; \\ \frac{2\lambda^2 \Delta z^2 \sigma^2}{L^4 \pi} (1 - \Omega^2 \sigma^2), & \frac{L}{\sigma} \gg 1. \end{cases} \quad (19)$$

The concurrence, denoted here by $\mathcal{C}_P(\rho_{AB})$ can be approximately expressed as

$$\mathcal{C}_P(\rho_{AB}) \approx \begin{cases} \frac{\lambda^2 \Delta z^2}{\sqrt{\pi}} \left(\frac{\sigma}{L^3} + \frac{1}{4L\sigma} - \frac{1}{3\sqrt{\pi}\sigma^2} + \frac{\Omega}{2\sigma} \right), & \frac{\Delta z}{\sigma} \ll \frac{L}{\sigma} \ll 1; \\ \max \left[0, -\frac{\lambda^2 \Delta z^2}{3\pi\sigma^2} + \frac{4\lambda^2 \Delta z^2 \sigma^2}{L^4 \pi} \right] = 0, & \frac{\Delta z}{\sigma} \ll 1, \frac{L}{\sigma} \gg 1. \end{cases} \quad (20)$$

Eq. (20) shows that the concurrence vanishes in the limit of $\Delta z \rightarrow 0$, i.e, the two detectors are located at the boundary, as well as when $L/\sigma \gg 1$, i.e., the interdetector separation is very large. This means that entanglement harvesting cannot occur in these cases. While

for small interdetector separation ($L/\sigma \ll 1$), the harvested entanglement is an increasing function of the energy gap (Ω) and the detector-to-boundary distance (Δz).

In the far zone to the boundary ($\Delta z/\sigma \gg 1$), one can also approximately estimate the concurrence

$$\mathcal{C}_P(\rho_{AB}) \approx \begin{cases} \frac{\lambda^2}{2\sqrt{\pi}} \left(\frac{\sigma}{L} - \frac{1}{\sqrt{\pi}} + \frac{\sigma^2}{2\sqrt{\pi}\Delta z^2} + \Omega\sigma \right), & \frac{\Delta z}{\sigma} \gg 1, \frac{L}{\sigma} \ll 1; \\ 0, & \frac{\Delta z}{\sigma} \gg \frac{L}{\sigma} \gg 1; \end{cases} \quad (21)$$

In the case of $L/\sigma \ll 1$, the concurrence is now a decreasing function of Δz , which is in contrast to the case of the near zone to the boundary where the concurrence is a growing function of Δz (see Eq. (20)). Therefore, one can infer that the amount of harvested entanglement ought to peak at a certain distance between the detectors and the boundary. This is what has been demonstrated in the numerical evaluations in Ref. [16].

2. Large energy gap

When the detectors' energy gap is much larger than the Heisenberg energy ($\Omega \gg 1/\sigma$), one can easily deduce from Eq. (15) that the concurrence should be vanishingly small. For such identical detectors near the boundary with not too large separation ($\Delta z/\sigma \ll 1, L/\sigma \ll 1$) the concurrence quantifying the harvested entanglement reads approximately,

$$\mathcal{C}_P(\rho_{AB}) \approx \frac{\lambda^2 e^{-\Omega^2 \sigma^2} \Delta z^2 \sigma}{L^3 \sqrt{\pi}}, \quad (22)$$

As a result, the harvested entanglement degrades to zero as the energy gap increases.

3. Numerical estimation

In order to gain a better understanding of the entanglement harvesting for nonidentical detectors with different energy gaps in the presence of the reflecting boundary, we now resort to numerical calculation since analytical approximations are hard to obtain in generic cases. We first show the results from our numerical evaluation on the role played by the reflecting boundary on entanglement harvesting in Figs. (2) and (3).

In Fig. (2), the amount of acquired entanglement is plotted as a function of interdetector separation for various detectors' energy gaps. Obviously, the harvested entanglement

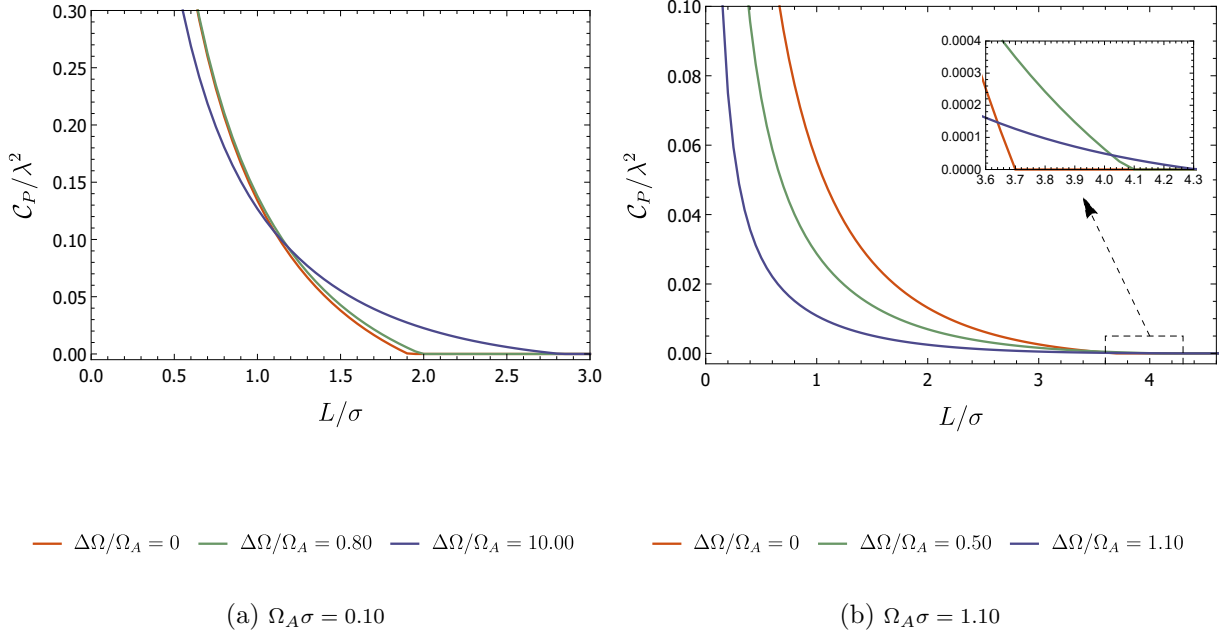


FIG. 2: The concurrence \mathcal{C}_P as a function of interdetector separation L/σ is plotted for $\Omega_A\sigma = 0.10$, $\Delta\Omega/\Omega_A = \{0, 0.80, 10.00\}$ in (a) and $\Omega_A\sigma = 1.10$, $\Delta\Omega/\Omega_A = \{0, 0.50, 1.10\}$ in (b) with fixed $\Delta z/\sigma = 1.00$.

monotonically degrade with the increasing interdetector separation no matter whether the two detectors are identical or not. For a fixed distance Δz from the boundary, the identical detectors usually have an advantage in acquiring more entanglement than nonidentical detectors with unequal energy gaps (e.g., see Fig. (2b)). In contrast, when the energy gaps are small and the interdetector separation is large enough with respect to the duration time parameter ($\Omega_A\sigma < \Omega_B\sigma \ll 1$ and $L > \sigma$), the nonidentical detectors are instead more likely to harvest more entanglement [see Fig. (2a)]. Notice that there is only a finite harvesting-achievable range for the interdetector separation for entanglement harvesting, which can be enlarged by a large energy gap (or energy gap difference).

In Fig. (3), we show how the presence of the boundary influences entanglement harvesting by plotting the concurrence as a function of $\Delta z/\sigma$ for various detectors' energy gaps. It is easy to see that the amount of harvested entanglement is zero in the limit of $\Delta z \rightarrow 0$ and approaches to their corresponding values in flat spacetime without any boundaries as $\Delta z \rightarrow \infty$ as expected. No matter whether the two detectors are nonidentical with different

energy gaps or identical, the harvested entanglement measure by concurrence has a peak value when the distance Δz is comparable to the duration time σ [e.g., see Fig. (3a)]. The exact position of detectors where the harvested entanglement peaks is not sensitive to the energy gap difference. Moreover, the reflecting boundary plays a double-edged role in entanglement harvesting (inhibiting the entanglement harvesting near the boundary or enhancing it when $\Delta z/\sigma > 1$ as compared to the case without any boundaries), regardless of whether the detectors are identical or not. Furthermore, both the amount of harvested entanglement and the influence of the boundary can be suppressed by increasing detectors' energy gaps or the energy gap difference between the two detectors.

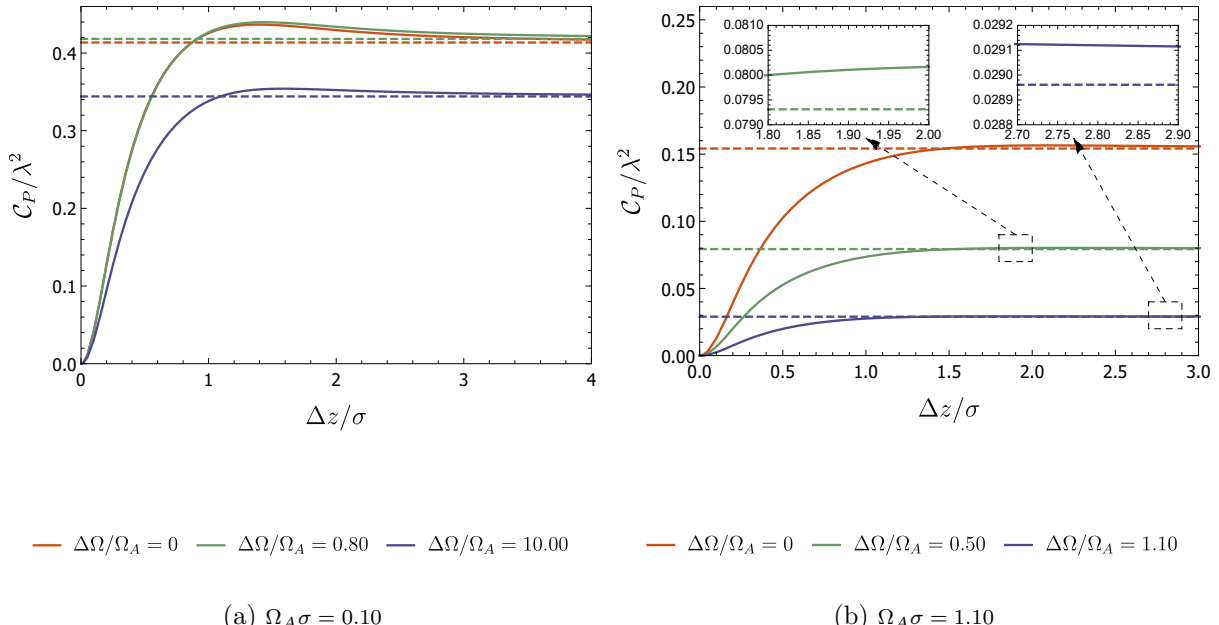


FIG. 3: The concurrence is plotted as a function of the distance $\Delta z/\sigma$ for fixed $L/\sigma = 0.50$. We assume $\Omega_A\sigma = 0.10$, $\Delta\Omega/\Omega_A = \{0, 0.80, 10.00\}$ in (a), and $\Omega_A\sigma = 1.10$, $\Delta\Omega/\Omega_A = \{0, 0.50, 1.10\}$ in (b). All the colored dashed lines correspondingly represent the results in flat spacetime without any boundaries, i.e., the results in the limit of $\Delta z \rightarrow \infty$.

In order to further study how the entanglement harvesting phenomenon for two nonidentical detectors depends on the energy gap difference, we plot concurrence as a function of the energy gap difference in Fig. (4). When the interdetector separation L is small relative to the duration time σ , the energy gap difference would generally hinder harvesting of entan-

lement, i.e., the harvested entanglement would rapidly degrade to zero with the increasing energy gap difference between two nonidentical detectors[see and Fig. (4a)]. However, when the interdetector separation grows to comparable to or larger than the interaction duration time parameter, i.e., $L \gtrsim \sigma$, the concurrence is no longer a monotonically decreasing function of the energy gap difference but may initially increase with the increasing energy gap difference, and then reach a maximum value at certain nonzero energy gap difference before degrade to zero as the energy gap difference further increases. [see and Fig. (4b)]. This suggests that there exist an optimal energy gap difference that maximizes the amount of entanglement harvested, which we denote by $\Delta\Omega_C$. It seems that the value of $\Delta\Omega_C$ depends upon both the interdetector separation and the detector-to-boundary distance. In order to analyze this clearly, we demonstrate how the value of the optimal energy gap difference is influenced by the presence of the boundary for various interdetector separations in Fig. (5). Obviously, the optimal energy gap difference is an increasing function of $\Delta z/\sigma$. i.e., the presence of the boundary reduces the optimal energy gap difference for entanglement harvesting. It is also easy to find the larger the interdetector separation, the larger the optimal value of the energy gap difference, which is consistent with the conclusion in Ref. [25].

B. Mutual information harvesting

Now, we begin to study mutual information harvesting. For identical detectors, the harvested mutual information can also be approximated in two cases: small energy gap and large energy gap.

1. Small energy gap

When the detectors system is placed near the boundary (i.e., $\Delta z/\sigma \ll 1$), the correlation term C is approximately given by

$$C \approx \begin{cases} \frac{\lambda^2 \Delta z^2}{2\pi\sigma^2} \left(\frac{1}{3} - \frac{L^2}{15\sigma^2} - \frac{\sqrt{\pi}\Omega\sigma}{2} \right), & \frac{L}{\sigma} \ll 1; \\ \frac{\lambda^2 \Delta z^2}{\pi} \left(\frac{2\sigma^2}{L^4} - \frac{\sqrt{\pi}\Omega}{4\sigma} e^{-\frac{L^2}{4\sigma^2}} \right), & \frac{L}{\sigma} \gg 1, \end{cases} \quad (23)$$

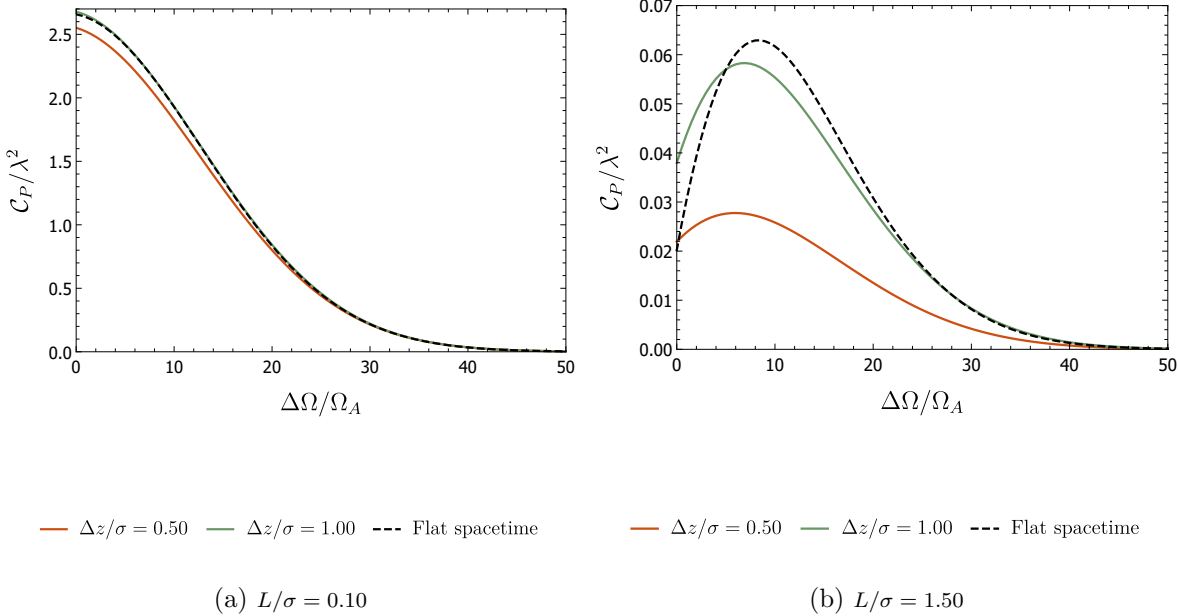


FIG. 4: The concurrence as a function of $\Delta\Omega/\Omega_A$ with $\Omega_A\sigma = 0.10$ for various $\Delta z/\sigma$. We assume $L/\sigma = 0.10$ in (a) and $L/\sigma = 1.50$ in (b). Here, the dashed line in all plots indicates the results in flat spacetime without any boundaries. There is a probability that nonidentical detectors may harvest more entanglement than the identical ones for large interdetector separation.

then the harvested mutual information can be approximated as

$$\mathcal{I}_P(\rho_{AB}) \approx \begin{cases} \frac{\ln 2}{3} \frac{\lambda^2 \Delta z^2}{\pi \sigma^2} + \frac{\lambda^2 L^2 \Delta z^2}{15\pi \sigma^4} \ln \left(\frac{L}{\sigma} \right) - \frac{\ln 2}{2} \frac{\lambda^2 \Omega \Delta z^2}{\sqrt{\pi} \sigma}, & \frac{\Delta z}{\sigma} \ll \frac{L}{\sigma} \ll 1; \\ \frac{12\lambda^2 \Delta z^2 \sigma^6}{L^8 \pi} (2 + 3\sqrt{\pi} \Omega \sigma), & \frac{\Delta z}{\sigma} \ll 1, \frac{L}{\sigma} \gg 1. \end{cases} \quad (24)$$

As can be seen from Eq. (24), the mutual information harvested by identical detectors, in the limit of $\Delta z \rightarrow 0$, i.e., the detectors are located at the boundary, must vanish. While, as the detector-to-boundary distance Δz increases, the mutual information grows like Δz^2 in the near zone of the boundary. It is also interesting to note that the harvested mutual information is a decreasing function of the detectors' energy gap Ω in the case of $L/\sigma \ll 1$, while it is an increasing function of the energy gap in the case of $L/\sigma \gg 1$. This is similar to the behavior for the mutual information harvesting in flat spacetime without any boundaries [3].

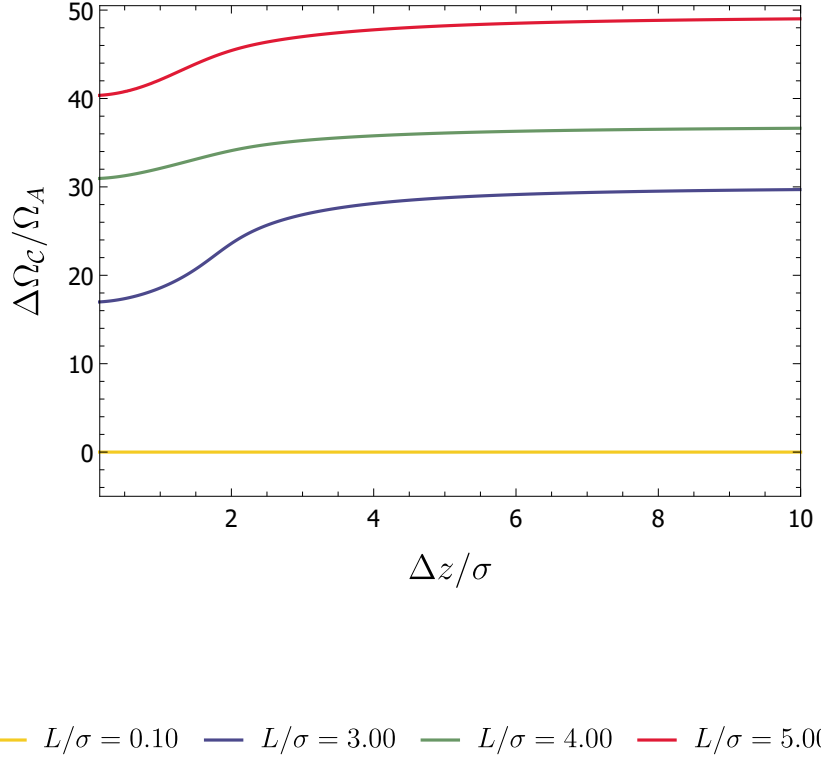


FIG. 5: The plot of $\Delta\Omega_C/\Omega_A$ versus $\Delta z/\sigma$ for two detectors aligned parallel to the boundary. Here, we set $\Omega_A\sigma = 0.10$ and $L/\sigma = \{0.10, 3.00, 4.00, 5.00\}$. It is apparent that $\Delta\Omega_C/\Omega_A$ is an increasing function of $\Delta z/\sigma$ as long as the interdetector separation is not too small with respect to the interaction duration time.

For $\Omega\sigma \ll 1$ and $\Delta z/\sigma \gg 1$, the harvested mutual information can be approximated as,

$$\mathcal{I}_P(\rho_{AB}) \approx \begin{cases} \frac{\lambda^2}{2\pi} \left[\ln 2 + \frac{L^2}{6\sigma^2} \ln \left(\frac{L}{\sigma} \right) - \frac{\sigma^2}{2\Delta z^2} \ln 2 - \sqrt{\pi}\Omega\sigma \ln 2 \right], & \frac{\Delta z}{\sigma} \gg 1, \frac{L}{\sigma} \ll 1; \\ \frac{\lambda^2\sigma^4}{L^2\pi} \left(\frac{1}{L^2} - \frac{1}{2\Delta z^2} + \frac{\sqrt{\pi}\Omega\sigma}{L^2} \right), & \frac{\Delta z}{\sigma} \gg \frac{L}{\sigma} \gg 1. \end{cases} \quad (25)$$

Eq. (25) shows that the amount of harvested mutual information is an increasing function of Δz , and its boundary dependence is of minus Δz^{-2} . The harvested mutual information is also a decreasing function of Ω in the case of $L/\sigma \ll 1$, but becomes an increasing function of Ω in the case of $L/\sigma \gg 1$. In the limit of $\Delta z \rightarrow \infty$, the Wightman function (12) reduces to that in flat spacetime, and so the harvested correlations (mutual information or entan-

lement) approach to the corresponding results in flat spacetime without any boundaries as expected.

2. Large energy gap

When the detectors' energy gap is much larger than the Heisenberg energy ($\Omega \gg 1/\sigma$), the mutual information for two identical detectors near the boundary with not too large separation ($\Delta z/\sigma \ll 1, L/\sigma \ll 1$) reads approximately

$$\mathcal{I}_P(\rho_{AB}) \approx \frac{\lambda^2 e^{-\Omega^2 \sigma^2} \Delta z^2}{8\pi \Omega^6 \sigma^{10}} \left[2\Omega^2 \sigma^4 \ln 2 - L^2 \ln(\Omega\sigma) \right]. \quad (26)$$

One can see that the harvested mutual information degrades to zero as the energy gap increases.

3. Numerical estimation

In more general cases, the mutual information harvesting behavior can be captured by resorting to numerical estimations. In Figs. (6) and (7), the amount of mutual information is plotted as a function of interdetector separation and detectors-to-boundary distance for various detectors' energy gaps, respectively. Obviously, similar to the entanglement, the harvested mutual information is also a monotonically decreasing function of the interdetector separation no matter whether the two detectors are identical or not. Interestingly, when the energy gaps are small and the interdetector separation is large enough with respect to the duration time parameter ($\Omega_A \sigma < \Omega_B \sigma \ll 1$ and $L > \sigma$), the nonidentical detectors with unequal energy gaps are likely to harvest more mutual information than the identical detectors [see Fig. (6a)], contrary to the usual wisdom that the identical detectors may be advantageous in mutual information harvesting. It should be pointed out that, unlike entanglement harvesting, mutual information can be harvested by two static detectors with an arbitrarily large interdetector separation, and physically, this means that the mutual information harvested outside the harvesting-achievable range of entanglement is either classical correlation or nondistillable entanglement [3].

Fig. (7) demonstrates that in the limit of $\Delta z \rightarrow \infty$ the mutual information approaches to its corresponding values in flat spacetime without any boundaries, while on the boundary the

mutual information vanishes as expected. In sharp contrast to the entanglement harvesting phenomenon which displays a peak-value behaviour when the distance Δz is comparable to the duration time σ [see Fig. (3)], the harvested mutual information is always a monotonically increasing function of $\Delta z/\sigma$, approaching asymptotically to the value without any boundaries. So, this means that the reflecting boundary always plays an inhibiting role in mutual information harvesting in contrast to its double-edged role in entanglement harvesting (inhibiting the entanglement harvesting near the boundary and enhancing it when $\Delta z/\sigma > 1$). Moreover, both the amount of harvested mutual information and the influence of the boundary can be suppressed by increasing detectors' energy gaps or the energy gap difference between the two detectors.

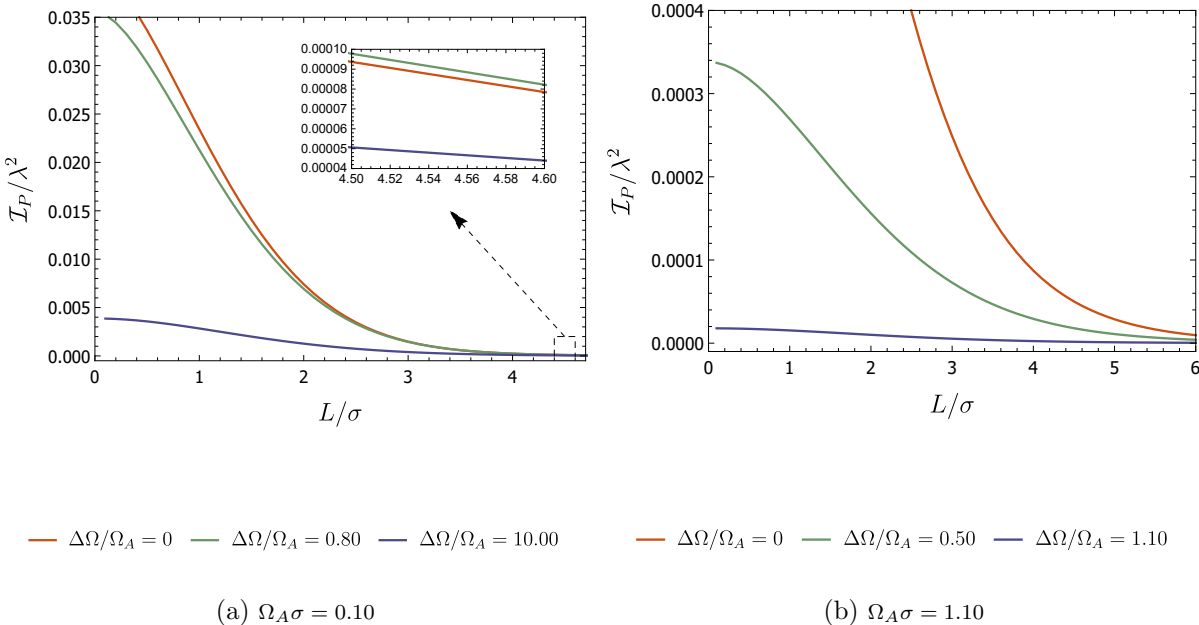


FIG. 6: The plots of mutual information \mathcal{I}_P versus the interdetector separation L/σ . Here, we have set $\Omega_A\sigma = 0.10$, $\Delta\Omega/\Omega_A = \{0, 0.80, 10.00\}$ in (a) and $\Omega_A\sigma = 1.10$, $\Delta\Omega/\Omega_A = \{0, 0.50, 1.10\}$ in (b) with fixed $\Delta z/\sigma = 1.00$.

In order to further investigate the influence of the energy gap difference on mutual information harvesting, we plot mutual information as a function of the energy gap difference in Fig. (8). Similar to entanglement harvesting, the harvested mutual information is also a monotonically decreasing function of the energy gap difference when the interdetector sep-

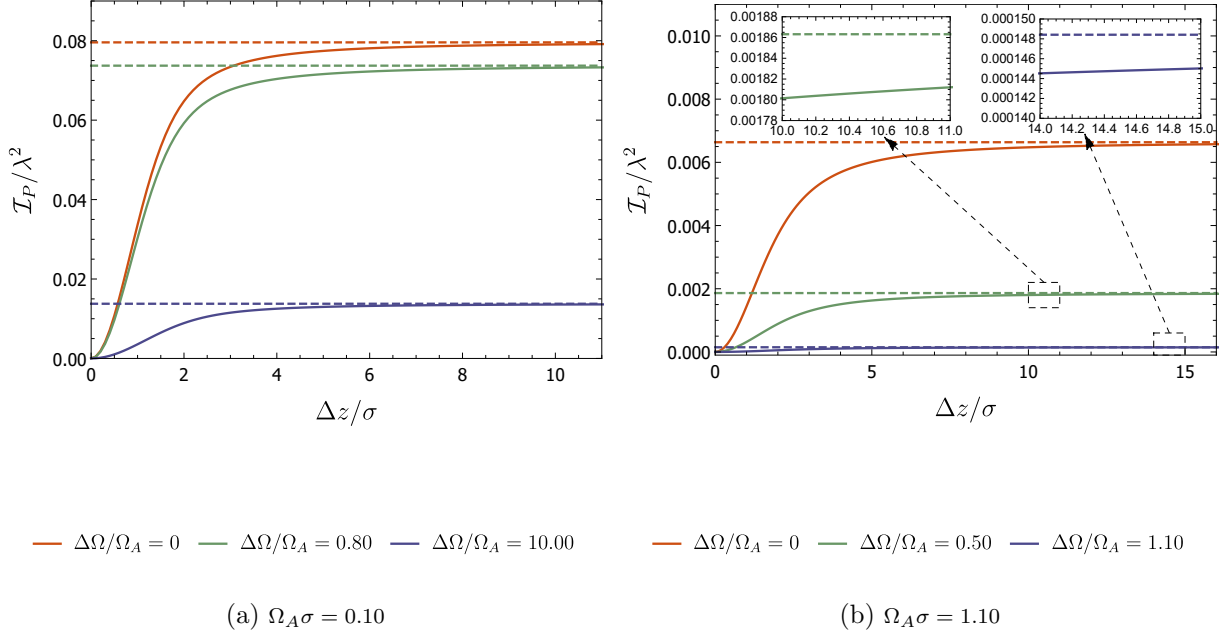


FIG. 7: The mutual information is plotted as the function of $\Delta z/\sigma$ with $\Omega_A\sigma = 0.10$, $\Delta\Omega/\Omega_A = \{0, 0.80, 10.00\}$ in (a), and $\Omega_A\sigma = 1.10$, $\Delta\Omega/\Omega_A = \{0, 0.50, 1.10\}$ in (b). Here, we have set $L/\sigma = 0.50$. The corresponding results in flat spacetime without any boundaries are shown as dashed lines.

aration is timelike and very small relative to the duration time σ [see Fig. (8a)]. However, when the interdetector separation is spacelike ($L \gg \sigma$), the mutual information is no longer a monotonically decreasing function of the energy gap difference but may peak at a certain nonzero energy gap difference and then degrade to zero with the increase of the energy gap difference [see Fig. (8b)], i.e., there also exists an optimal energy gap difference that maximizes the mutual information. We demonstrate how the optimal energy gap difference, denoted here by $\Delta\Omega_{\mathcal{I}}$, depends upon the presence of the boundary in Fig. (9). Analogous to that in the case of entanglement harvesting, the optimal energy gap difference $\Delta\Omega_{\mathcal{I}}$ generally increases as the interdetector separation increases. However, the presence of the boundary can either increase or decrease the optimum energy gap difference for mutual information harvesting. Specifically, when the interdetector separation is large with respect to the duration time, the optimum energy gap difference for mutual information harvesting is an increasing function of the detector-to-boundary distance; however, when the interdetector

separation grows to too large, the optimum energy gap difference for mutual information harvesting becomes a decreasing function rather than an increasing function of the detector-to-boundary distance, which is quite different from that in entanglement harvesting.

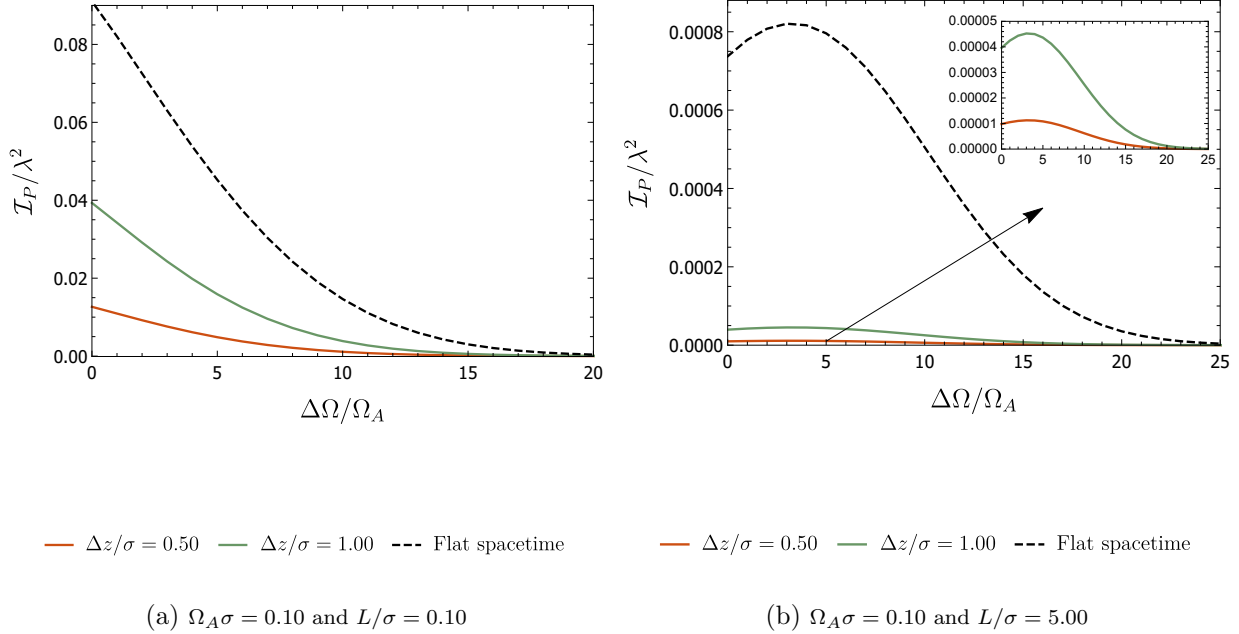


FIG. 8: Mutual information is plotted as a function of $\Delta\Omega/\Omega_A$ for various fixed $\Delta z/\sigma$ with $\Omega_A\sigma = 0.10$ and $L/\sigma = 0.10$ in (a) and a spacelike interdetector separation $L/\sigma = 5.00$ in (b). Here, the dashed line denotes the results in flat spacetime without any boundaries. Plot (b) shows that for large interdetector separation the nonidentical detectors may harvest more mutual information than identical detectors.

It is well known that once there is a reflecting plane boundary in flat spacetime, the isotropy of spacetime would be lost. Therefore, the orientation of two detectors system in various angular alignment with respect to the boundary may have a non-negligible impact on correlation harvesting. So, in the next section, we will consider the situation in which the two detectors are aligned vertically to the boundary plane.

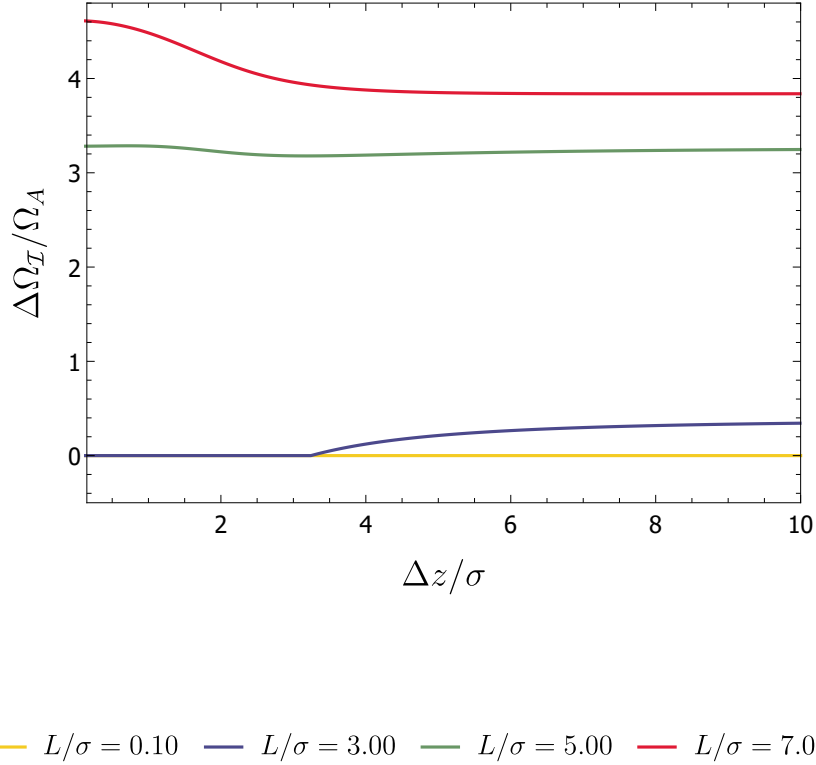


FIG. 9: The plot of $\Delta\Omega_I/\Omega_A$ versus $\Delta z/\sigma$ with $\Omega_A\sigma = 0.10$, $L/\sigma = \{0.10, 3.00, 5.00, 7.00\}$ for two detectors aligned parallel to the boundary.

IV. CORRELATION HARVESTING FOR THE DETECTORS ALIGNED VERTICALLY TO THE BOUNDARY

The spacetime trajectories of two static detectors aligned vertically to the boundary can be written as [see Fig. (10)]

$$x_A := \{t_A, x = 0, y = 0, z = \Delta z\}, \quad x_B := \{t_B, x = 0, y = 0, z = \Delta z + L\}. \quad (27)$$

Substituting Eq. (12) and Eq. (27) into Eq. (4), we can see that P_A is just the expression of Eq. (13), and P_B can be obtained by replacing Δz with $\Delta z + L$ in Eq. (13). Similarly, the correlation terms C and X can be calculated out

$$C = \frac{\lambda^2}{4\sqrt{\pi}} e^{-\frac{\Delta\Omega^2\sigma^2}{4}} \left[f(L) - f(L + 2\Delta z) \right], \quad (28)$$

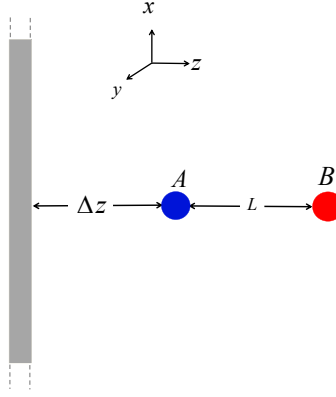


FIG. 10: Two static detectors are separated by a distance L aligned vertically to the boundary plane and Δz is the distance between the boundary and the detector which is closer.

$$X = -\frac{\lambda^2}{4\sqrt{\pi}} e^{-\frac{(2\Omega_A + \Delta\Omega)^2 \sigma^2}{4}} \left[g(L) - g(L + 2\Delta z) \right], \quad (29)$$

with auxiliary functions $f(L)$ and $g(L)$ defined by Eq.(16) and Eq. (17), respectively. According to Eq. (7) and Eq. (9), the concurrence and harvested mutual information can be directly obtained.

A. Entanglement harvesting

The approximate expressions for the concurrence for identical detectors can be also obtained in some special cases.

1. Small energy gap

For small energy gap ($\Omega\sigma \ll 1$), the concurrence, denoted here by $\mathcal{C}_V(\rho_{AB})$, can be shown after some long algebraic manipulations to take the following approximate form

$$\mathcal{C}_V(\rho_{AB}) \approx \begin{cases} \frac{\lambda^2 \Delta z}{\sqrt{\pi}} \left(\frac{\sigma}{L^2} + \frac{1}{4\sigma} - \frac{L}{3\sqrt{\pi}\sigma^2} + \frac{L\Omega}{2\sigma} \right), & \frac{\Delta z}{\sigma} \ll \frac{L}{\sigma} \ll 1; \\ \frac{\lambda^2}{2\sqrt{\pi}} \left(\frac{\sigma}{L} - \frac{1}{\sqrt{\pi}} + \frac{\sigma^2}{2\sqrt{\pi}\Delta z^2} + \Omega\sigma \right), & \frac{\Delta z}{\sigma} \gg 1, \frac{L}{\sigma} \ll 1; \\ 0, & L \gg \sigma. \end{cases} \quad (30)$$

Similar to the case of parallel-to-boundary alignment, Eq. (30) demonstrates that the entanglement cannot be extracted at extremely large interdetector separation L or vanishing

distance Δz from the boundary. Comparing Eq. (30) with Eqs. (20) and (21), we can find for $\Delta z/\sigma \ll 1$ the harvested entanglement in the vertical-to-boundary scenario is also an increasing function of Δz , but the boundary dependence behaves like Δz rather than Δz^2 , while for $\Delta z/\sigma \gg 1$ the approximate form of concurrence in both the vertical-to-boundary and parallel-to-boundary alignment looks the same and behaves as a decreasing function of Δz . This non-monotonicity of a function with respect to Δz implies that the harvested entanglement in the vertical-to-boundary case also possesses a peak behavior. Beside these, one may find that the detectors aligned vertically to boundary can harvest comparatively more entanglement than these in parallel-to-boundary alignment for the case of $\Delta z \ll L \ll \sigma$. This is physically in accordance with our finding the boundary inhibits the entanglement harvesting for the detectors close to it.

2. Large energy gap

For large energy gap ($\Omega \gg 1/\sigma$), the concurrence in the case of $\Delta z/\sigma \ll 1$ and $L/\sigma \ll 1$ can be approximated as

$$\mathcal{C}_V(\rho_{AB}) \approx \frac{\lambda^2 e^{-\Omega^2 \sigma^2} \Delta z \sigma}{L^2 \sqrt{\pi}}. \quad (31)$$

Similar to the case of the parallel-to-boundary alignment, the harvested entanglement in the vertical-to-boundary alignment also degrade with the increasing detectors' energy gap.

3. Numerical estimations

From above approximations, it is easy to infer that the influence of the boundary on the entanglement harvesting phenomenon for two detectors aligned vertically to the boundary should be similar to that for two detectors aligned parallel to the boundary, i.e., qualitatively, the reflecting boundary should play an a double-edge role (inhibiting entanglement harvesting for $\Delta z \ll \sigma$ and assisting entanglement harvesting for $\Delta z > \sigma$), and moreover, entanglement harvesting possesses a finite harvesting-achievable range regardless of the presence of the boundary. However, the quantitative details should be slightly different. To better understand it, we define the difference of concurrence between the scenarios of vertical-to-boundary and parallel-to-boundary alignments: $\Delta \mathcal{C} := \mathcal{C}_V - \mathcal{C}_P$.

The difference in the amount of harvested entanglement is plotted as a function of the

distance from the boundary in Fig. (11). As we can see from Fig. (11), the detectors in vertical-to-boundary alignment near the boundary ($\Delta z/\sigma \ll 1$) could harvest comparatively more entanglement than that in parallel-to-boundary alignment. However, when the detectors are located far from the boundary ($\Delta z/\sigma \gg 1$) with not too large interdetector separation, this would be reversed, i.e., the parallel-to-boundary alignment turns out to be favorable for entanglement harvesting. This is because the boundary would play a strongly inhibiting role in entanglement harvesting for two detectors placed near the boundary, and the detectors system in vertical-to-boundary alignment has a relatively longer effective distance from the boundary and thus less inhibiting effect, resulting in more entanglement harvested in comparison with those in parallel-to-boundary alignment. While when two detectors are far away from the boundary, the assisting role played by the boundary leads to more entanglement harvested by detectors in parallel-to-boundary alignment in comparison to vertical-to-boundary alignment.

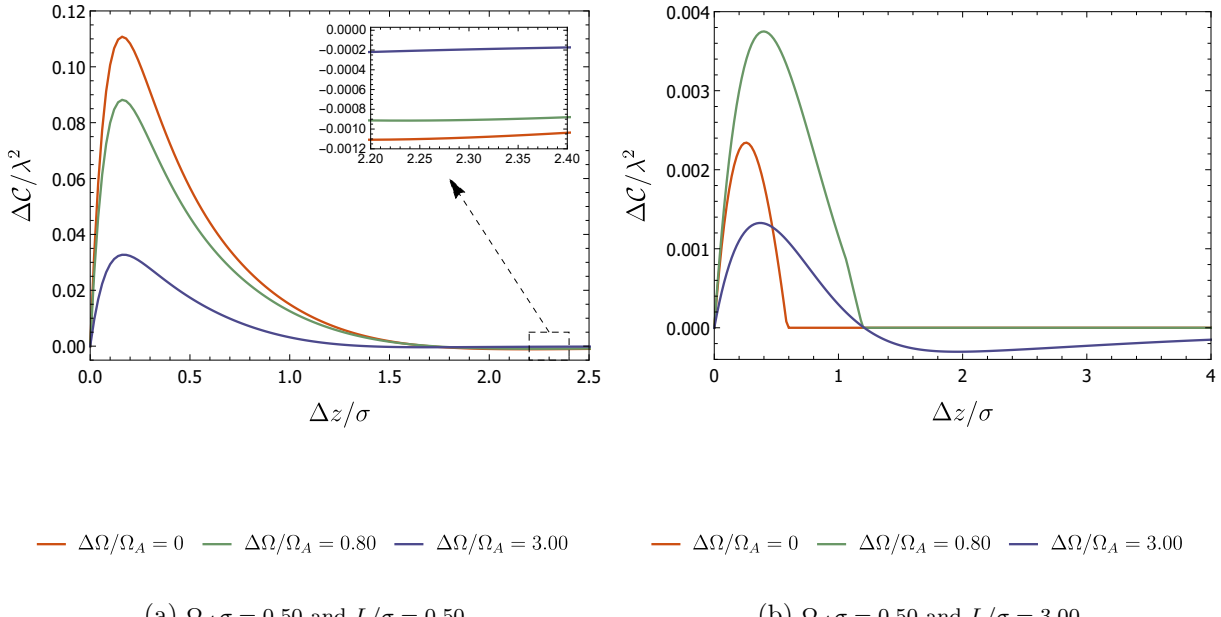


FIG. 11: The concurrence difference $\Delta\mathcal{C}$ between vertical-to-boundary and parallel-to-boundary alignments, is plotted as a function of the distance $\Delta z/\sigma$. Here, we have fixed $L/\sigma = 0.50$ in plot (a) and $L/\sigma = 3.00$ in plot (b). In all plots, we have set $\Omega_A\sigma = 0.50$ with $\Delta\Omega/\Omega_A = \{0, 0.80, 3.00\}$.

In Fig (12), we demonstrate how the optimal energy gap difference that maximizes the

amount of harvested entanglement depends upon the detector-to-boundary distance. It is easy to find that the optimal energy gap difference $\Delta\Omega_C$ in vertical-to-boundary alignment is also an increasing function of the detector-to-boundary distance, but the quantitative detail is slightly different from that in the scenario of parallel-to-boundary alignment [comparing Fig (12) and Fig. (5)].

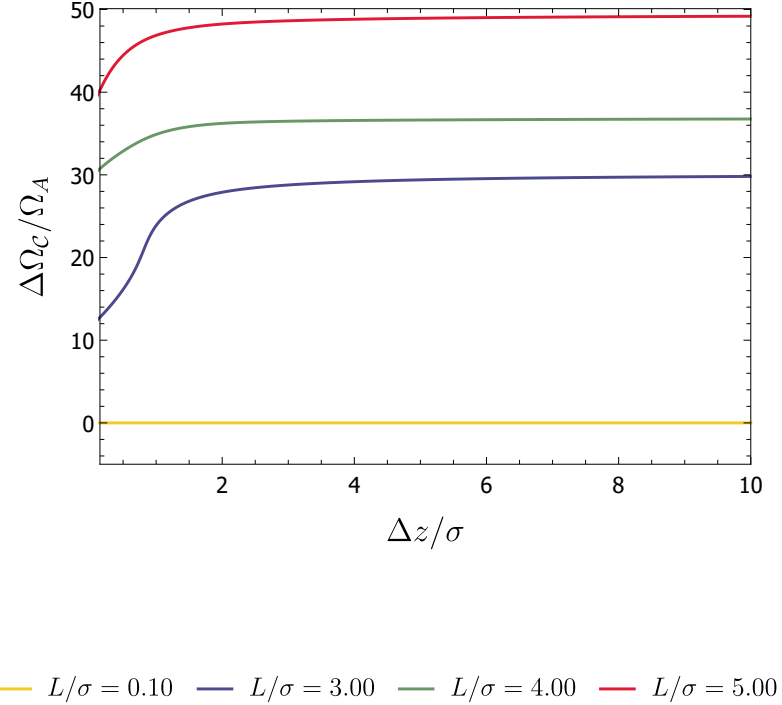


FIG. 12: The plot of $\Delta\Omega_C/\Omega_A$ versus $\Delta z/\sigma$ with $\Omega_A\sigma = 0.10$ and $L/\sigma = \{0.10, 3.00, 4.00, 5.00\}$ for two detectors in vertical-to-boundary alignment.

B. Mutual information harvesting

Now we are in a position of estimating the mutual information harvested by detectors aligned vertically to the boundary. Similarly, the analytical approximation of mutual information can also be obtained for identical detectors in some special cases.

1. Small energy gap

For small energy gap ($\Omega\sigma \ll 1$), the mutual information denoted here by $\mathcal{I}_V(\rho_{AB})$ in vertical-to-boundary alignment can be approximated as

$$\mathcal{I}_V(\rho_{AB}) \approx \begin{cases} \frac{\lambda^2(2-3\sqrt{\pi}\Omega\sigma)\Delta z^2}{6\pi\sigma^2} \ln\left(\frac{L}{\Delta z}\right), & \frac{\Delta z}{\sigma} \ll \frac{L}{\sigma} \ll 1; \\ \frac{32\lambda^2(1+\sqrt{\pi}\Omega\sigma)\sigma^4\Delta z^2}{L^6\pi} \ln\left(\frac{\sigma}{\Delta z}\right), & \frac{\Delta z}{\sigma} \ll 1, \frac{L}{\sigma} \gg 1; \\ \frac{\lambda^2}{2\pi} \left[\ln 2 + \frac{L^2}{6\sigma^2} \ln\left(\frac{L}{\sigma}\right) - \frac{\sigma^2}{2\Delta z^2} \ln 2 - \sqrt{\pi}\Omega\sigma \ln 2 \right], & \frac{\Delta z}{\sigma} \gg 1, \frac{L}{\sigma} \ll 1; \\ \frac{\lambda^2\sigma^4}{L^2\pi} \left(\frac{1}{L^2} - \frac{1}{2\Delta z^2} + \frac{\sqrt{\pi}\Omega\sigma}{L^2} \right), & \frac{\Delta z}{\sigma} \gg 1, \frac{L}{\sigma} \gg 1. \end{cases} \quad (32)$$

In comparison with Eq. (24), the boundary dependence of mutual information, in the case $\Delta z/\sigma \ll 1$, is $\Delta z^2 \ln(\sigma/\Delta z)$ in vertical-to-boundary alignment, rather than Δz^2 in parallel-to-boundary alignment. Hence, the detectors aligned vertically to the boundary would harvest more mutual information than those aligned parallel to the boundary in the near zone of the boundary. Physically, we can understand it as follows. Since the reflecting boundary always inhibits the harvesting of mutual information as previously discovered, the vertical-to-boundary alignment has a comparatively larger effective detector-to-boundary distance than the parallel-to-boundary alignment, so the detectors aligned vertically to the boundary could harvest more mutual information. When compared with Eq. (25) for $\Delta z/\sigma \gg 1$, the approximated expressions of Eq. (32) have the same form as that of Eq. (25), which in the limit of $\Delta z \rightarrow \infty$ reduce to the result in flat Minkowski spacetime, which is isotropic, as expected.

2. Large energy gap

For large energy gap ($\Omega \gg 1/\sigma$), the mutual information in the case of $\Delta z/\sigma \ll 1$ and $L/\sigma \ll 1$ can be approximated as

$$\mathcal{I}_V(\rho_{AB}) \approx \frac{\lambda^2 e^{-\Omega^2\sigma^2} \Delta z^2}{4\pi\Omega^4\sigma^6} \ln(L/\Delta z). \quad (33)$$

Obviously, the harvested mutual information in vertical-to-boundary alignment will degrade to zero as the energy gap grows.

3. Numerical estimations

With the above discussions, it is easy to infer that the influence of the boundary on the mutual information harvesting phenomenon for two detectors aligned vertically to the boundary should be similar to that for two detectors aligned parallel to the boundary, i.e., qualitatively, the reflecting boundary should always play an inhibiting role in mutual information harvesting, and moreover mutual information can be harvested at arbitrarily large interdetector separation. However, the quantitative details may in general be slightly different. To better understand it, we define the difference of mutual information between the scenarios of vertical-to-boundary and parallel-to-boundary alignments: $\Delta\mathcal{I} := \mathcal{I}_V - \mathcal{I}_P$.

The difference in the amount of harvested mutual information is plotted, in Fig. (13), as a function of the distance between the boundary and the detector which is closer. As we can see from Fig. (13), the case of vertical-to-boundary alignment in general is more favorable for mutual information harvesting than that of parallel-to-boundary alignment. This is because the boundary always plays an inhibiting role in mutual information harvesting and the case of vertical-to-boundary alignment has relatively longer effective distance from boundary.

In addition, the boundary dependence for the optimal energy gap difference between two nonidentical detectors that maximizes the amount of mutual information is displayed in Fig. (14). Similar to the case of parallel-to-boundary alignment, the optimal energy gap difference $\Delta\Omega_{\mathcal{I}}$ in the case of vertical-to-boundary alignment can be either an increasing or a decreasing function of detector-to-boundary distance Δz . Specifically, when the interdetector separation is large with respect to the duration time, the optimum energy gap difference $\Delta\Omega_{\mathcal{I}}$ is an increasing function of Δz ; however, when the interdetector separation is too large, $\Delta\Omega_{\mathcal{I}}$ becomes a decreasing function of Δz .

V. CONCLUSION

We have performed a detailed study on the phenomenon of correlations harvesting by a pair of UDW detectors interacting with vacuum scalar fields in flat spacetime with the presence of a perfectly reflecting boundary. The influences of the energy gaps, the energy gap difference and the presence of the boundary on the mutual information harvesting and entanglement harvesting for nonidentical detectors are examined in the scenarios of parallel-

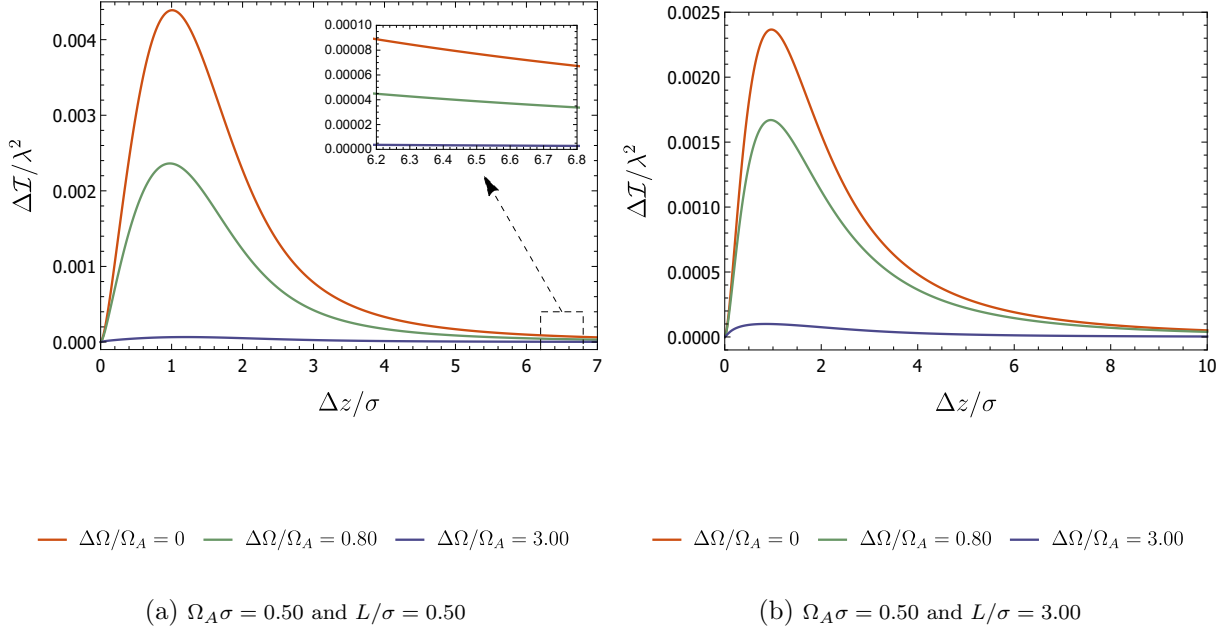


FIG. 13: The mutual information difference $\Delta\mathcal{I}$ is plotted as a function of the distance $\Delta z/\sigma$. Here, we have fixed $L/\sigma = 0.50$ in plot (a) and $L/\sigma = 3.00$ in plot (b). In all plots, we have set $\Omega_A\sigma = 0.50$ with $\Delta\Omega/\Omega_A = \{0, 0.80, 3.00\}$.

to-boundary and vertical-to-boundary alignments.

For the case of parallel-to-boundary alignment, both the harvested entanglement and mutual information decrease as the interdetector separation increases, and they are also exponentially suppressed by increasing the detectors' energy gaps. It is worth pointing out the entanglement harvesting phenomenon possesses only a finite harvesting-achievable range for interdetector separation, which can be enlarged by increasing the detectors' energy gaps (or energy gap difference), while mutual information, in contrast, can be extracted at an arbitrary interdetector separation with an infinite harvesting-achievable range. Moreover, when detectors are located near the boundary ($\Delta z \rightarrow 0$), both mutual information harvesting and entanglement harvesting are inhibited. However, as the distance to the boundary grows to infinity, the harvested mutual information always increases, finally approaching to the corresponding value in flat spacetime without any boundaries. In contrast, the harvested entanglement will surpass the corresponding value in flat spacetime without any boundaries at a certain distance and peak when the distance becomes comparable to the duration

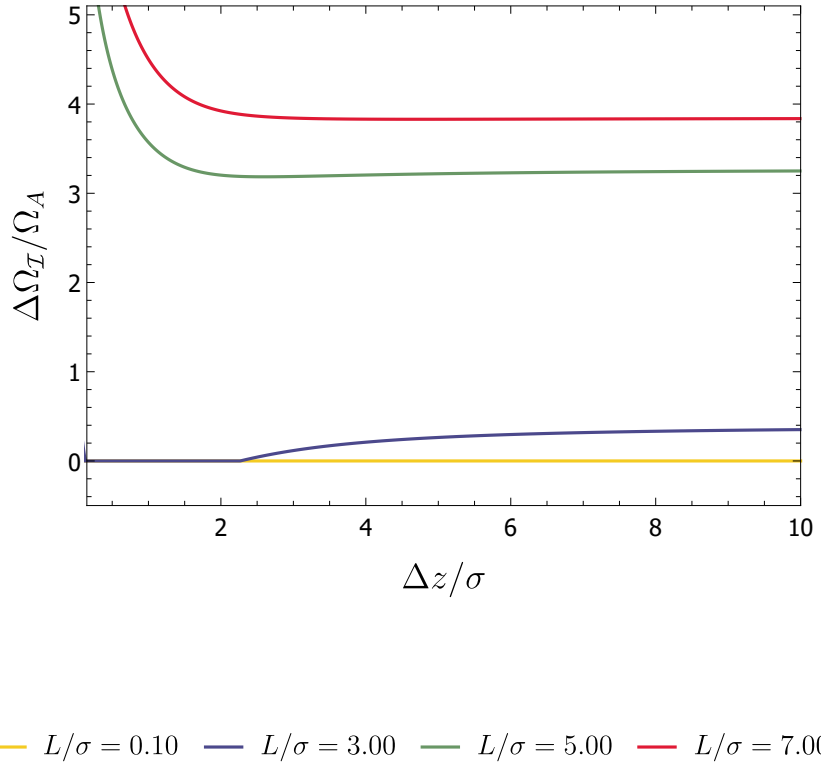


FIG. 14: The plot of $\Delta\Omega_I/\Omega_A$ versus $\Delta z/\sigma$ with $\Omega_A\sigma = 0.10$ and $L/\sigma = \{0.10, 3.00, 5.00, 7.00\}$ for two detectors in vertical-to-boundary alignment.

time parameter before turn to decrease and ultimately approach to the corresponding value in flat spacetime without any boundaries when the distance becomes infinite, no matter whether the two detectors are identical or not. Hence, the reflecting boundary, in the sense of correlations harvesting, always plays an inhibiting role in mutual information harvesting but a double-edged role in entanglement harvesting in contrast.

When the interdetector separation is small with respect to the duration time, the harvested correlations are a monotonically decreasing function of the energy gap difference no matter whether the boundary exists or not, i.e., identical detectors will be advantageous to extracting correlations as compared to nonidentical detectors with different energy gaps. However, for not too small interdetector separation, the amount of both harvested entanglement and mutual information possess a maximum value at a certain nonzero energy gap difference, suggesting that there is an optimal value of energy gap difference between two

nonidentical detectors which renders the detectors to harvest most correlations. The optimal energy gap difference generally increases as the interdetector separation increases. Interestingly, the presence of the boundary always decreases the value of the optimal energy gap difference for entanglement harvesting, while it can either increase or decrease the optimum energy gap difference for mutual information harvesting. To be specific, the optimum energy gap difference for mutual information harvesting may be decreased by the presence of the boundary when the interdetector separation is large with respect to the duration time, and be increased when the interdetector separation grows to too large.

As for the vertical-to-boundary alignment case, the influence of energy gaps and the boundary on both entanglement harvesting and mutual information harvesting is qualitatively similar to that for parallel-to-boundary alignment case, and only quantitative details are slightly different. Specifically, the detectors system in vertical-to-boundary alignment always harvest comparatively more mutual information than the parallel-to-boundary ones, while they harvest comparatively more entanglement only near the boundary. This can be understood physically as a result of that the detectors system in vertical-to-boundary alignment has a longer effective distance to the boundary.

Acknowledgments

This work was supported in part by the NSFC under Grants No.12075084 and No.12175062, and Postgraduate Scientific Research Innovation Project of Hunan Province under Grant No.CX20220507.

Appendix A: The derivations of C and X in parallel-to-boundary alignment

1. The correlation term C

Letting $u = \tau$ and $s = \tau - \tau'$, we have, after carrying out the integration with respect to u in Eq. (5),

$$C = \lambda^2 \sqrt{\pi} \sigma e^{-\sigma^2(\Omega_A - \Omega_B)^2/4} \int_{-\infty}^{\infty} ds e^{-\frac{s^2 + 2is\sigma^2(\Omega_A + \Omega_B)}{4\sigma^2}} W(s) . \quad (\text{A1})$$

Considering the detectors' trajectories (11), one can obtain the corresponding Wightman function

$$W(s) = -\frac{1}{4\pi^2} \left[\frac{1}{(s - i\epsilon)^2 - L^2} - \frac{1}{(s - i\epsilon)^2 - L^2 - 4z^2} \right]. \quad (\text{A2})$$

Then the correlation term C takes the form

$$C = C_0 - C_z, \quad (\text{A3})$$

with

$$C_0 = -\frac{\lambda^2 \sigma}{4\pi^{3/2}} e^{-\Delta\Omega^2 \sigma^2/4} \int_{-\infty}^{\infty} \frac{e^{-s^2/(4\sigma^2)}}{(s - i\epsilon)^2 - L^2} e^{-i(2\Omega_A + \Delta\Omega) \cdot s/2} ds, \quad (\text{A4})$$

and

$$C_z = -\frac{\lambda^2 \sigma}{4\pi^{3/2}} e^{-\Delta\Omega^2 \sigma^2/4} \int_{-\infty}^{\infty} \frac{e^{-s^2/(4\sigma^2)}}{(s - i\epsilon)^2 - L^2 - 4z^2} e^{-i(2\Omega_A + \Delta\Omega) \cdot s/2} ds, \quad (\text{A5})$$

where $\Delta\Omega := \Omega_B - \Omega_A$. Using the Sokhotski formula,

$$\frac{1}{x \pm i\epsilon} = \mathcal{P} \frac{1}{x} \mp i\pi\delta(x), \quad (\text{A6})$$

we have

$$\begin{aligned} C_0 &= -\frac{\lambda^2 \sigma}{4\pi^{3/2}} e^{-\Delta\Omega^2 \sigma^2/4} \mathcal{P} \int_{-\infty}^{\infty} \frac{e^{-s^2/(4\sigma^2)}}{s^2 - L^2} e^{-i(2\Omega_A + \Delta\Omega) \cdot s/2} ds \\ &\quad - \frac{i\lambda^2 \sigma}{4\pi^{1/2}} e^{-\Delta\Omega^2 \sigma^2/4} \int_{-\infty}^{\infty} e^{-s^2/(4\sigma^2)} e^{-i(2\Omega_A + \Delta\Omega) \cdot s/2} \text{sgn}(s) \delta(s^2 - L^2) ds \\ &= -\frac{\lambda^2 \sigma e^{-\Delta\Omega^2 \sigma^2/4}}{4\pi^{3/2}} \mathcal{P} \int_{-\infty}^{\infty} \frac{e^{-i(2\Omega_A + \Delta\Omega) \cdot s/2} e^{-s^2/(4\sigma^2)}}{s^2 - L^2} ds - \frac{\lambda^2 \sigma e^{-\frac{\Delta\Omega\sigma^4 + L^2}{4\sigma^2}}}{4\sqrt{\pi}L} \sin \left[\frac{(2\Omega_A + \Delta\Omega)L}{2} \right], \end{aligned} \quad (\text{A7})$$

where $\text{sgn}(s)$ represents the sign function. The integration in the last line of Eq. (A7) can be performed straightforwardly by using the convolution of two functions in Fourier transforms, i.e.,

$$\begin{aligned} &\quad -\frac{\lambda^2 \sigma}{4\pi^{3/2}} e^{-\Delta\Omega^2 \sigma^2/4} \mathcal{P} \int_{-\infty}^{\infty} \frac{e^{-s^2/(4\sigma^2)}}{s^2 - L^2} e^{-i(2\Omega_A + \Delta\Omega) \cdot s/2} ds \\ &= \frac{\lambda^2 \sigma}{4\sqrt{\pi}L} e^{-(L^2 + \Delta\Omega^2 \sigma^4)/(4\sigma^2)} \text{Im} \left[e^{i(2\Omega_A + \Delta\Omega)L/2} \text{Erf} \left(\frac{iL + 2\Omega_A \sigma^2 + \Delta\Omega \sigma^2}{2\sigma} \right) \right]. \end{aligned} \quad (\text{A8})$$

Then C_0 can be expressed in the form

$$C_0 = \frac{\lambda^2}{4\sqrt{\pi}} e^{-\frac{\Delta\Omega^2 \sigma^2}{4}} f(L) \quad (\text{A9})$$

with

$$f(L) := \frac{\sigma e^{-L^2/(4\sigma^2)}}{L} \left\{ \text{Im} \left[e^{i(2\Omega_A + \Delta\Omega)L/2} \text{Erf} \left(\frac{iL + 2\Omega_A\sigma^2 + \Delta\Omega\sigma^2}{2\sigma} \right) \right] - \sin \left[\frac{(2\Omega_A + \Delta\Omega)L}{2} \right] \right\}. \quad (\text{A10})$$

Comparing the integration in Eq. (A4) with that in Eq. (A5), we easily obtain the expression of C_z from C_0 with L replaced by $\sqrt{L^2 + 4\Delta z^2}$

$$C_z = \frac{\lambda^2}{4\sqrt{\pi}} e^{-\frac{\Delta\Omega^2\sigma^2}{4}} f(\sqrt{L^2 + 4\Delta z^2}). \quad (\text{A11})$$

Therefore, combining Eqs. (A9) and (A11) can verify the validity of Eq. (14).

2. The correlation term X

Upon considering $W(x_A(\tau'), x_B(\tau)) = W(x_B(\tau'), x_A(\tau))$, the expression of Eq. (6) can be simplified as

$$\begin{aligned} X &= -\lambda^2 \int_{-\infty}^{\infty} du \chi(u) \chi(u-s) e^{-i(\Omega_A + \Omega_B)u} \int_0^{\infty} ds \left[e^{i\Omega_A s} W(-s) + e^{i\Omega_B s} W(-s) \right] \\ &= -\lambda^2 \sqrt{\pi} \sigma e^{-\frac{\sigma^2(\Omega_A + \Omega_B)^2}{4}} \int_0^{\infty} ds e^{-\frac{s^2}{4\sigma^2}} \left[e^{is\frac{\Omega_A - \Omega_B}{2}} W(-s) + e^{-is\frac{\Omega_A - \Omega_B}{2}} W(-s) \right], \end{aligned} \quad (\text{A12})$$

where $u = \tau$ and $s = \tau - \tau'$ are introduced.

Inserting the Wightman function (A2) into Eq. (A12), we have

$$X = X_0 - X_z, \quad (\text{A13})$$

with

$$X_0 := \frac{\lambda^2 \sigma}{2\pi^{3/2}} e^{-\sigma^2(2\Omega_A + \Delta\Omega)^2/4} \int_0^{\infty} \frac{e^{-s^2/(4\sigma^2)} \cos(s\Delta\Omega/2)}{(-s - i\epsilon)^2 - L^2} ds, \quad (\text{A14})$$

and

$$X_z = \frac{\lambda^2 \sigma}{2\pi^{3/2}} e^{-\sigma^2(2\Omega_A + \Delta\Omega)^2/4} \int_0^{\infty} \frac{e^{-s^2/(4\sigma^2)} \cos(s\Delta\Omega/2)}{(-s - i\epsilon)^2 - L^2 - 4\Delta z^2} ds. \quad (\text{A15})$$

Using the Sokhotski formula (A6), we find, after carrying out the fourier transformation, Eq. (A14) takes the form [25]

$$\begin{aligned} X_0 &= -\frac{\sigma \lambda^2 e^{-L^2/(4\sigma^2)}}{4L\sqrt{\pi}} e^{-\frac{(2\Omega_A + \Delta\Omega)^2\sigma^2}{4}} \left\{ \text{Im} \left[e^{i\Delta\Omega L/2} \text{Erf} \left(\frac{iL + \Delta\Omega\sigma^2}{2\sigma} \right) \right] + i \cos \left(\frac{\Delta\Omega L}{2} \right) \right\} \\ &= -\frac{\lambda^2}{4\sqrt{\pi}} e^{-\frac{(2\Omega_A + \Delta\Omega)^2\sigma^2}{4}} g(L) \end{aligned} \quad (\text{A16})$$

with

$$g(L) := \frac{\sigma e^{-L^2/(4\sigma^2)}}{L} \left\{ \text{Im} \left[e^{i\Delta\Omega L/2} \text{Erf} \left(\frac{iL + \Delta\Omega\sigma^2}{2\sigma} \right) \right] + i \cos \left(\frac{\Delta\Omega L}{2} \right) \right\}. \quad (\text{A17})$$

Similarly, X_z takes the following form

$$X_z = -\frac{\lambda^2}{4\sqrt{\pi}} e^{-\frac{(2\Omega_A + \Delta\Omega)^2\sigma^2}{4}} g(\sqrt{L^2 + 4\Delta z^2}). \quad (\text{A18})$$

Combining Eq. (A16) with Eq. (A18) gives Eq. (15).

[1] S. J. Summers and R. Werner, Phys. Lett. A **110**, 257 (1985).

[2] S. J. Summers and R. Werner, J. Math. Phys. (N.Y.) **28**, 2448 (1987).

[3] A. Pozas-Kerstjens and E. Martin-Martinez, Phys. Rev. D **92**, 064042 (2015).

[4] K. K. Ng, R. B. Mann, and E. Martin-Martinez, Phys. Rev. D **97**, 125011 (2018).

[5] M. Naeem, K. Gallock-Yoshimura, and R. B. Mann, Phys. Rev. D **107**, 065016 (2023).

[6] E. Martin-Martinez, A. R. H. Smith, and D. R. Terno, Phys. Rev. D **93**, 044001 (2016).

[7] G. L. Ver Steeg and N. C. Menicucci, Phys. Rev. D **79**, 044027 (2009).

[8] Y. Nambu, Entropy **15**, 1847 (2013).

[9] S. Kukita and Y. Nambu, Entropy **19**, 449 (2017).

[10] K. K. Ng, R. B. Mann, and E. Martin-Martinez, Phys. Rev. D **98**, 125005 (2018).

[11] L. J. Henderson, R. A. Hennigar, R. B. Mann, A. R. H. Smith, and J. Zhang, Classical Quantum Gravity **35**, 21LT02 (2018).

[12] L. J. Henderson, R. A. Hennigar, R. B. Mann, A. R. H. Smith, and J. Zhang, J. High Energy Phys. 05 (2019) 178.

[13] M. P. G. Robbins, L. J. Henderson, and R. B. Mann, arXiv:2010.14517 [hep-th].

[14] K. Gallock-Yoshimura, E. Tjoa, and R. B. Mann, Phys. Rev. D **104**, 025001 (2021).

[15] W. Cong, C. Qian, M. R. R. Good, and R. B. Mann, J. High Energy Phys. 10 (2020) 067.

[16] Z. Liu, J. Zhang, and H. Yu, J. High Energy Phys. 08 (2021) 020.

[17] W. Cong, E. Tjoa, and R. B. Mann, J. High Energy Phys. **06** (2019) 021.

[18] G. Salton, R. B. Mann, and N. C. Menicucci, New J. Phys **17**, 035001 (2015).

[19] J. Zhang and H. Yu, Phys. Rev. D **102**, 065013 (2020).

[20] Z. Liu, J. Zhang, R. B. Mann, and H. Yu, Phys. Rev. D **105**, 085012 (2022).

- [21] C. Suryaatmadja, W. Cong, and R. B. Mann, arXiv:2205.14739 [quant-ph].
- [22] H. Maeso-Garcia, T. Rick Perche, and E. Martin-Martinez, Phys. Rev.D **106**, 045014 (2022).
- [23] Z. Liu, J. Zhang, and H. Yu, Phys. Rev. D **107**, 045010 (2023).
- [24] L. J. Henderson, A. Belenchia, E. Castro-Ruiz, C. Budroni, M. Zych, Č. Brukner, and R. B. Mann, Phys. Rev. Lett. **125**, 131602 (2020).
- [25] H. Hu, J. Zhang, and H. Yu, J. High Energy Phys. 05 (2022) 112.
- [26] H. B. G. Casimir, Proc. K. Ned. Akad. Wet. **51**, 793(1948).
- [27] H. Yu and L. H. Ford, Phys. Rev. D **60**, 084023(1999).
- [28] H. Zhai, J. Zhang and H. Yu, Ann. Phys. (N. Y.) **371**, 338 (2016).
- [29] H. Yu and S. Lu, Phys. Rev. D **72**, 064022(2005).
- [30] H. Yu and Z. Zhu, Phys. Rev. D **74**, 044032 (2006).
- [31] L. Rizzato and S. Spagnolo, J. Phys. Conf. Ser. **161**, 012031 (2009).
- [32] J. Zhang and H. Yu, Phys. Rev. D **75**, 104014(2007).
- [33] J. Zhang and H. Yu, Phys. Rev. A **75**, 012101(2007).
- [34] S. Cheng, H. Yu and J. Hu, Phys. Rev. D **98**, 025001 (2018).
- [35] P. Simidzija and E. Martin-Martinez, Phys. Rev. D **98**, 085007 (2018).
- [36] K. Bueley, L. Huang, K. Gallock-Yoshimura, and R. B. Mann, Phys. Rev. D **106**, 025010(2022).
- [37] W. K. Wootters, Phys. Rev. Lett. **80**, 2245 (1997).
- [38] M. Nielsen and I. Chuang, Quantum Computation and Quantum Information(Cambridge University Press, Cambridge, England, 2000).
- [39] N. D. Birrell and P. C. W. Davies, Quantum Fields in Curved Space (Cambridge University Press, Cambridge, U.K.,1984).